Nuclear Engineering and Technology 52 (2020) 1565–1570

Contents lists available at ScienceDirect

Nuclear Engineering and Technology

journal homepage: www.elsevier.com/locate/net

Original Article

Enhanced photon shielding efficiency of a flexible and lightweight rare earth/polymer composite: A Monte Carlo simulation study

Ying Wang [a], Guangke Wang [c], Tao Hu [b], Shipeng Wen [b], Shui Hu [b, *], Li Liu [a, b, **]

[a] State Key Laboratory of Chemical Resource Engineering, Beijing University of Chemical Technology, Beijing 100029, China
[b] Beijing Engineering Research Center of Advanced Elastomers, Beijing University of Chemical Technology, Beijing 100029, China
[c] Global Energy Internet Research Institute Corporation Ltd, Beijing, 102211, China

ARTICLE INFO

Article history:
Received 24 October 2019
Received in revised form
24 December 2019
Accepted 29 December 2019
Available online 30 December 2019

Keywords:
Photon
Composite
Monte Carlo simulation
Rare earth

ABSTRACT

Photons with the energy of 60 keV are regularly used for some kinds of bone density examination devices, like the single photon absorptiometry (SPA). This article reports a flexible and lightweight rare earth/polymer composite for enhancing shielding efficiency against photon radiation with the energy of 60 keV. Lead oxide (PbO) and several rare earth element oxides (La_2O_3, Ce_2O_3, Nd_2O_3) were dispersed into natural rubber (NR) and the photon radiation shielding performance of the composites were assessed using monte carlo simulation method. For 60 keV photons, the shielding efficiency of rare earth-based composites were found to be much higher than that of the traditional lead-based composite, which has bad absorbing ability for photons with energies between 40 keV and 88 keV. In comparison with the lead oxide based composite, Nd_2O_3-NR composite with the same protection standard (the lead equivalent is 0.25 mmPb, 0.35 mmPb and 0.5 mmPb, respectively), can reduce the thickness by 35.29%, 37.5% and 38.24%, and reduce the weight by 38.91%, 40.99% and 41.69%, respectively. Thus, a flexible, lightweight and lead-free rare earth/NR composite could be designed, offering efficient photon radiation protection for the users of the single photon absorptiometry (SPA) with certain energy of 60 keV.

1. Introduction

Photon radioactive sources have been widely used in disease diagnostic and therapeutic applications [1–5]. Unwanted exposures to photon radiation are hazardous to people's health, especially for long term exposure. To avoid hazard from these radiation sources, lead/rubber composites, which combine the good absorbing ability of lead for ionizing radiation [3,6–9] and the improved processing ability, good flexibility of rubber, have traditionally used as personnel radiation protection materials [1,3,10,11]. However, there is a weak absorption energy region between 40 and 88 keV [10,12], so called "lead feeble absorbing area", in which the photon (gamma ray) shielding efficiency of lead is low. Coincidentally, the energy of photon emitted from most of clinical diagnostic devices is below 100 keV [13,14]. As a result, the shielding polymer based composites filled with lead or lead compounds must be made much thicker or heavier by adding more filler to provide sufficient radiation protection [15]. Such heavy lead/polymer composites would cause discomfort and even back problems to the operators and patients. Moreover, another weakness of lead is its toxicity [10,14].

Consequently, research efforts have been focused on developing alternative materials for lead. A variety of shielding materials (e.g., concrete, iron, tantalum, barium, tungsten, tin, rare earths, or other high Z elements) have attracted tremendous attention as lead-free alternatives for attenuation or adsorption of the undesired radiations [15–19]. The shielding properties of these candidates have been proved better than that of lead just at some energy region due to their different K electron shells [1], but these candidates cannot replace lead at the wide energy region below 100 keV.

In order to offer broad spectrum protection, researchers have designed multilayer structural radiation shielding materials contained multiple metal elements [20–22]. As-fabricated shielding material is much lighter and thinner than typical lead-based material or non-Pb materials which mixed various high Z elements as

* Corresponding author. Beijing Engineering Research Center of Advanced Elastomers, Beijing University of Chemical Technology, Beijing, 100029, China.
** Corresponding author. Beijing Engineering Research Center of Advanced Elastomers, Beijing University of Chemical Technology, Beijing, 100029, China.
E-mail addresses: hushui@mail.buct.edu.cn (S. Hu), liul@mail.buct.edu.cn (L. Liu).

https://doi.org/10.1016/j.net.2019.12.028

functional filler. However, the shortcoming of these multilayer composites is their complicated manufacturing process, which leads to high production cost and low products' qualified rate.

We suggest another study approach that our research can be focused toward designing efficient, flexible, lightweight and cost-effective shielding materials for protection only against certain energy of radiation encountered in specific medical device instead of broad-spectrum protection. For example, single photon absorptiometry (SPA), one of clinical examination device for bone metabolism disease, just release 60 keV photons emitted from its ^{241}Am source [23,24]. The photonic shielding performance of the shielding materials can be optimized by making use of the absorption edge. In this regard, rare earths whose absorption energy of the K-shell electron between 38.9 and 63.3 keV [10], have become best candidates that can be designed to effective attenuate radiation emitted from the ^{241}Am source of SPA.

In this paper, based on photon shielding theory, monte-carlo simulation method is adopted to assess the photon radiation shielding performance of natural rubber (NR) composites filled with different kinds of rare earth element oxides (La_2O_3, Ce_2O_3, Nd_2O_3). Compared to traditional lead oxide/rubber composite, rare earths/rubber composites show much better photon radiation shielding ability. With the same protection property for 60 keV photons, the thickness and the weight of Nd_2O_3-NR composite was found to be reduced by 35.3% and 48.9% at least, respectively. In other words, rare earths/rubber composites will be much lighter, safer and more flexible. Therefore, it provides a new approach for reducing weight or thickness of the radiation composites used as personnel radiation protection materials for clinical diagnostic devices emitted photons with mono energetic radiation.

2. Materials and methods

2.1. Theoretical calculations

Attenuation of photons in shielding materials can be expressed by the next equation:

$$I = I_0 \exp(-\mu x) \tag{1}$$

where I_0 and I represent the incident and transmitted photon intensities respectively, μ is linear attenuation coefficient and x is thickness of shielding material. A straight line can be obtained with thickness as the abscissa and $\ln\frac{I}{I_0}$ as the ordinate. The slope of the straight line is μ [25]. The larger the μ is, the better the shielding performance of the material will be.

There is another parameter can be determined using the following equation:

$$\mu_m = \frac{\mu}{\rho} \tag{2}$$

where μ_m is mass attenuation coefficient [26] and ρ is density of material. The larger the μ_m is, the better the shielding performance of the material will be. The μ_m of composite can be calculated by the next equation:

$$\mu_m = \Sigma w_i \left(\frac{\mu}{\rho}\right)_i \tag{3}$$

where w_i represents the mass fraction of component in the composite [27].

Photon shielding rate can be denoted as SR and determined as follows:

$$SR = 1 - \exp(-\mu x) \tag{4}$$

Obviously, the larger the SR is, the better the shielding performance of the material will be. Besides, by means of formula (2) and (3), SR can be described using another equation:

$$SR = 1 - \exp(-\mu_m M) \tag{5}$$

where M represents the mass of per unit area of the shielding material. The required mass of a certain material can be calculated by formula (5) when reached a certain shielding rate.

The required thickness of the shielding material to attenuate the beam intensity to 50% of the incident intensity is called half-value layer (*HVL*) [28]. It can be written as follows:

$$HVL = \frac{ln2}{\mu} \tag{6}$$

Similarly, the required thickness of the shielding material to attenuate the beam intensity to 10% of the incident intensity is called ten-value layer (*TVL*) [29]. It can be written by the next equation:

$$TVL = \frac{ln10}{\mu} \tag{7}$$

The smaller the *HVL* and *TVL*, the better the shielding performance of the material.

2.2. Experiment

Monte carlo simulation MCNP is a computer algorithm based on random sampling. The radiation source is defined by inputting incident particle type, energy, geometric position and incident direction. During the simulation, the incident particles are tracked by probability statistics. After a particle passing through the transmission plane, it stops tracking and starts to simulate the next particle until all the particles are simulated. The distribution of particle intensity and dose can be obtained by means of the data recorded by the detectors during the tracking process.

The simulate geometric model is shown in Fig. 1. Photons with certain energy are vertically shoot into the flat shielding material along the positive direction of the z-axis. It is assumed that the material is ideal with uniform distribution of components. It has stable geometry without shrinkage and expansion. The composites with different filler are denoted as La_2O_3-NR, Ce_2O_3-NR, Nd_2O_3-NR and PbO-NR, respectively.

To assess the photon radiation shielding performance of different composites, the energy of radiation source is defined changing from 35 to 95 keV. Then by means of defining thickness of composites as 0.02, 0.04, 0.06, 0.08 and 0.1 cm, the shielding performance of rare earth element oxides and lead oxide under 60 keV energy photons which emitted from ^{241}Am of SPA can be further

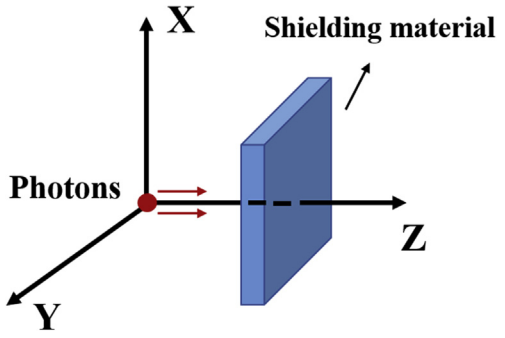

Fig. 1. Geometric structure of the simulates.

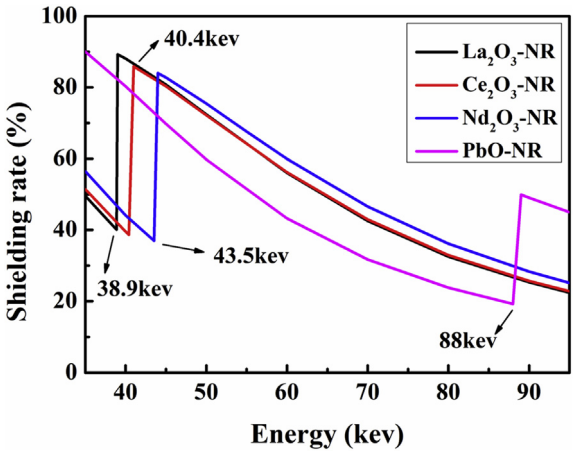

Fig. 2. Shielding rates under different energies.

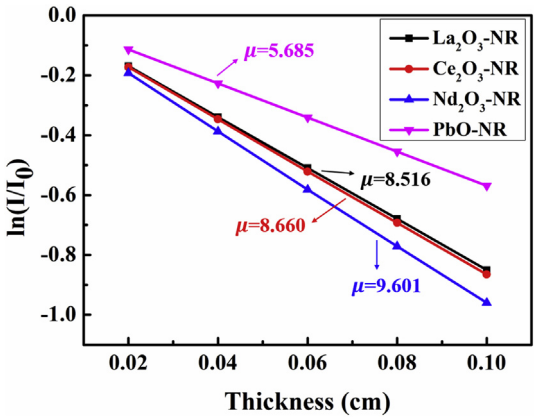

Fig. 3. Linear fitting.

compared.

In order to research influence of thickness and filler content on shielding performance, shielding filler with best property selected out based on above study is simulated under the photon of 60 keV. Five different thicknesses of 0.2, 0.4, 0.6, 0.8, and 1.0 cm are defined respectively and a series of different filler contents are defined for each thickness.

For the purposes of verifying the reliability of the simulation model, the best shielding filler is simulated under the photon of 60 keV and the mass fractions of the filler are 0, 0.1, 0.2, 0.3, 0.4, 0.5 and 0.6, respectively. The μ_m of NR and Nd_2O_3 are obtained by National institute of standards and technology (NIST) and formula (3) and the shielding rate at different masses is calculated by formula (5). The theoretical calculated values are compared with the simulated values.

3. Results and discussion

3.1. Comparison of photon shielding performance

Curves of shielding rate changes along with photon energy are illustrated in Fig. 2. The K shell absorption edges of La, Ce, Nd and Pb are 38.9, 40.4, 43.5 and 88 keV. The shielding rate decreased with the energy increasing but increased sharply when the photon energy reached the K shell absorption edge and then decreased again. This is because when the photon energy is low, the material absorbs photons mainly through the photoelectric effect. The greater the probability of photoelectric effect, the more rays are absorbed and the better the shielding performance. The probability of the photoelectric effect is inversely proportional to the third power of the photon energy. Therefore, the probability of photoelectric effect and the shielding rate decreased with the energy increasing. When the incident energy is exactly equal to the K shell absorption edge of the shielding element, the photon energy will be completely absorbed by the electron and the probability of photoelectric effect is greatly increased. So the shielding rate will increase sharply near the K shell absorption edge. In addition, the probability of photoelectric effect is also proportional to the fourth power of the atomic number of shielding element. The atomic number of lead is bigger than rare earths, so the shielding rate of PbO is better than other compounds outside lead feeble absorbing area but worse in this area because of the K shell absorption edge of rare earth elements. Therefore, the rare earth elements can replace lead to increase the protection effect when the photon energy is in the lead feeble absorbing area.

As shown in Fig. 3, A straight line can be obtained with the thickness as the abscissa and $\ln\frac{I}{I_0}$ as the ordinate. The μ of four composites can get from the slope of the straight lines respectively.

The *HVL* and *TVL* of each composite can be further calculated from μ. The obtained values of μ, *HVL* and *TVL* at defined energy (60 keV) are illustrated in Fig. 4(a). The abscissa represents different composites, the left ordinate represents the values of μ and the right ordinate represents the values of *HVL* and *TVL*. In terms of

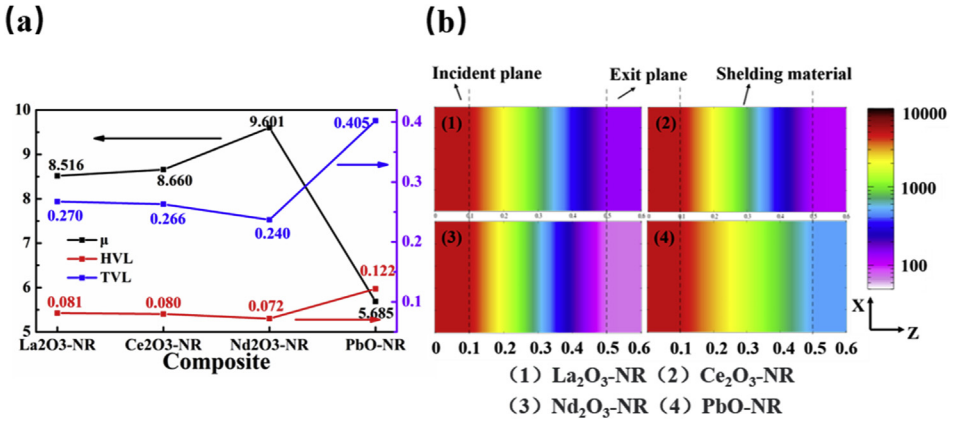

Fig. 4. Comparison of shielding properties of composites with different fillers.

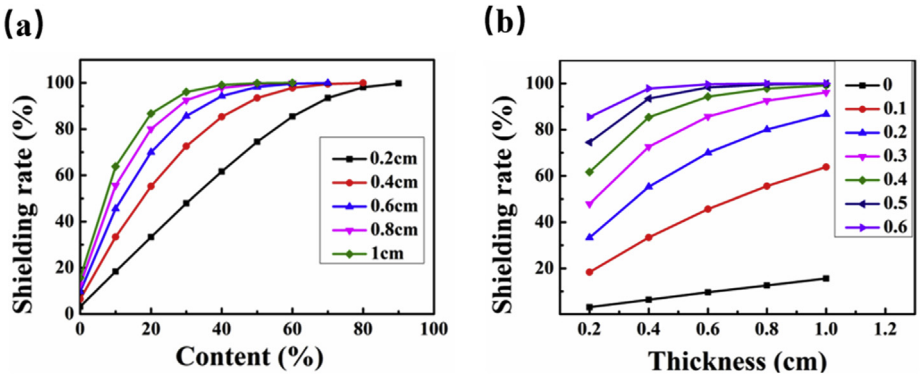

Fig. 5. Curves of shielding rate change with the increasing filler content and thickness.

numerical values, the sequence of μ is Nd_2O_3-NR > Ce_2O_3-NR > La_2O_3-NR > PbO-NR, while the sequence of *HVL* or *TVL* is PbO-NR > La_2O_3-NR > Ce_2O_3-NR > Nd_2O_3-NR. The larger the μ is, or the smaller the *HVL* and *TVL* are, the better the shielding effect will be. Therefore, the shielding effect of La_2O_3, Ce_2O_3 and Nd_2O_3 is obviously better than that of PbO when the photon energy is 60 keV. It is because the closer the K shell absorption edge of the shielding material is to the photons' energy emitted from the source, the better the shielding effect will be. Among these four elements, the K shell absorption edge of Nd is closest to 60 keV, so it has the best shielding effect. Then Ce and La in turns and the Pb is last.

The particle distributions of the X-Z cross profile in four different composites are illustrated in Fig. 4(b) and the different colors represent different particle intensity. The photons shoot into the shielding material at 0.1 cm and exit at 0.5 cm. The figure indicates that the intensity decay continually as the particles passed through the shielding material. When leaved the PbO-NR composite, the photon intensity is obviously greater than that of other shielding materials. It indicates that the photon shielding efficiency of rare earth oxides is obviously better than lead oxide. In addition, the photon shielding efficiency of Nd_2O_3 is slightly higher than La_2O_3 and Ce_2O_3, which is consistent with the above conclusion.

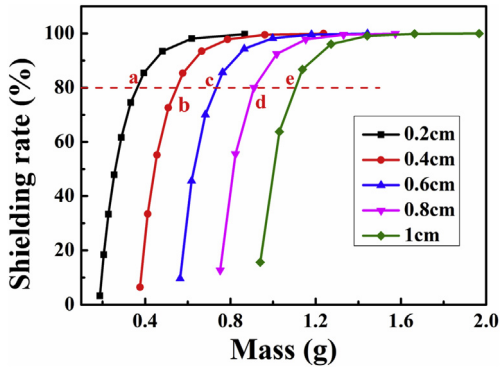

Fig. 6. Curves of shielding rate change with the increasing mass.

Table 1
The reduced weight of other points compared with the point e.

Site	Thickness/cm	Mass/g	⊿ M
a	0.2	0.36	67.57%
b	0.4	0.55	50.45%
c	0.6	0.74	33.33%
d	0.8	0.91	18.02%
e	1.0	1.11	–

3.2. Influence of thickness and filler content on shielding performance

Basing on the above research, Nd_2O_3 is selected as the functional filler to design shielding composite and the relationship between filler content or material thickness and shielding property is further studied. Fig. 5(a) illustrates the variation of shielding rate versus filler content for composites of different thickness at filler content from 0 to 1. Fig. 5(b) shows the curve of shielding rate versus thickness for composites containing different contents of Nd_2O_3 filler at thickness ranging from 0.2 cm to 1 cm. In Fig. 5(a), when the content of filler is zero, the shielding rate corresponds to the pure rubber matrix, while when the content reaches 100%, it corresponds to the pure Nd_2O_3. As the content of filler increased, the shielding rate increased rapidly in the begin then the growth rate slowed down. It is because when the content of filler is low, there are more blank microregions without effective shielding elements in the composite and these blank microregions will form photon transmission "channels", resulting in poor shielding performance. As the filler content increases, there will form filler network structure in the polymer matrix, leading the blank microregions decreased. Thus the shielding rate will increase rapidly. However, different from the simulation, with the increasing of filler content,

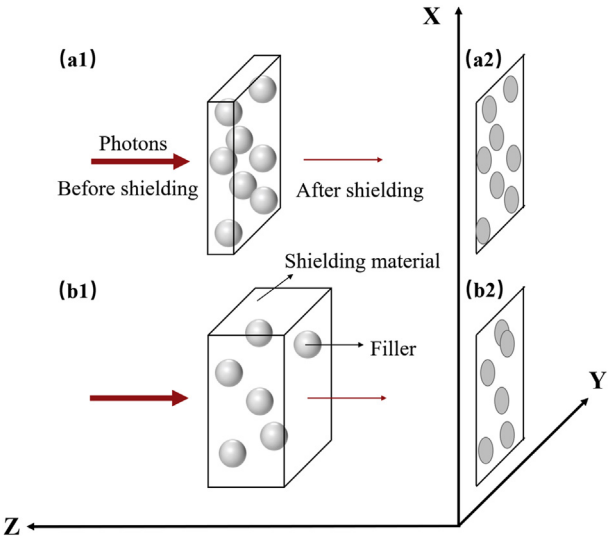

Fig. 7. Schematic diagram of composite for ray shielding.

the proportion of polymer matrix in the composite decreases gradually and the softness, mechanical properties and weight of the material will change in practical terms. Therefore, the comprehensive performance should be considered in the formulation design instead of pursuing the increase of filler content lonely.

In Fig. 5(b), as the thickness of material increased, the shielding rate increased rapidly in the begin and then the growth rate slowed down. It is because photons decay exponentially as they pass through the shielding material and that's shown in formula (1). Therefore, the shielding rate increased exponentially with thickness increasement. And the curves in Fig. 5(b) follow this trend.

The curves of shielding rate changes with the increasing mass of shielding material are shown in Fig. 6. As the mass of material increased (that is the thickness or filler content increased), the shielding rate increased rapidly in the begin then the growth rate slowed down. According to formula (5), the shielding rate increases exponentially with the mass increasing. And the curves in Fig. 6 follow this trend.

In addition, when materials of different thicknesses reached the same shielding rate, their mass can get from Fig. 6. For example, a horizontal straight line is made along the point whose shielding rate is 80%. The intersection points of the horizontal straight line and shielding rate curves denote as a, b, c, d and e respectively. From these points, mass of different materials can be obtained. The reduced weight of other points compared with the point e are shown in Table 1. When the thickness was 0.8 cm, 0.6 cm, 0.4 cm and 0.2 cm, the weight of materials decreased by 18.02%, 33.33%, 50.45% and 67.57%, respectively. That is the thinner material is lighter when reached the same shielding rate. It is because shielding effect mainly depends on material thickness and collision probability between photons and effective shielding elements. The greater the collision probability and thickness, the greater the photon attenuation and then the better the shielding effect. Fig. 7 is a schematic diagram of composite for ray shielding. Material (a1) and (b1) have the same shielding rate. Compared with (b1), (a1) is thinner and the filler content is higher. Figure (a2) and (b2) represent the projection of the two materials on the incident direction of the photon respectively, and the shaded parts represent the fillers. As shown in the figure, material with higher content of filler has a larger projection area of fillers and then the collision probability between effective shielding elements and photons is greater, so the shielding efficiency is higher. On the contrary, material with lower content of filler has lower shielding efficiency and in order to achieve the same shielding rate, it is necessary to increase its thickness. The weight increase caused by thickness far exceeds the filler content. So when reach the same shielding rate, the material with less filler content has greater thickness and weight. Therefore, in order to reduce the weight of protective material, the content of filler should be increased as much as possible on the premise of ensuring other properties meeting the requirements.

Based on the above data and conclusions, the Nd_2O_3 and the traditional photon shielding filler PbO are set as the filler respectively. The thickness of the two different materials can be obtained when reached different lead equivalent. Furthermore, the percentage of thickness and weight reduced by Nd_2O_3 compared with traditional protective composite can be calculated. And the data are shown in Table 2. According to Table 2, when the protective composite reached 0.25mmPb, the thickness and weight of Nd_2O_3 material are reduced by 35.29% and 38.91% compared with traditional materials. When reached 0.35mmPb and 0.5mmPb, the thickness of Nd_2O_3 material are reduced by 37.5% and 38.24% and the mass are reduced by 40.99% and 41.69%. It can be seen that when Nd_2O_3 is selected as the shielding filler, the thickness and weight of the protective composite can be greatly reduced while guaranteeing the protective performance.

Table 2
Thickness of two materials and reduced thickness and weight by Nd_2O_3.

Security Level of Protection Suit	Lead Equivalent/ mmPb	Thickness of Shielding Materials/ cm		Percentage Reduction/%	
		PbO	Nd_2O_3	⊿ T	⊿ M
I	0.25	0.17	0.11	35.29%	38.91%
II	0.35	0.24	0.15	37.5%	40.99%
III	0.5	0.34	0.21	38.24%	41.69%

3.3. Comparison between theory and simulation

The μ_m of NR and Nd_2O_3 can get from the NIST and that of the composites with different filler contents can be calculated by formula (3). The shielding rate of composites can get from formula (5). Fig. 8 represents the curves of theoretical calculation and simulation. The figure shows that small differences exist between theory and simulation and the theoretical values slightly greater than simulation values. That may be because each element distributed uniformly according to their mass fraction on atomic scale in the simulation and it is totally different from the actual particle distribution. The theoretical volume is smaller than simulative volume so the theoretical density is bigger than simulative density. And that leads theoretical μ_m which closely related to density bigger than simulative μ_m, then resulting in shielding performance of theory is better than that of simulation. But in general, the error between simulation and theoretical calculation is within the acceptable range, so the simulation model is reliable.

4. Conclusions

In the lead feeble absorbing area, the photon shielding performance of rare earth oxide is obviously better than that of PbO. Nd_2O_3 is the best, followed by Ce_2O_3 and La_2O_3. The higher the filler content is, the smaller the thickness and weight needed when reach a certain shielding rate. When reach different lead equivalent, the protective material Nd_2O_3-NR reduced the thickness by 35.29%, 37.5% and 38.24%, and reduced the weight by 38.91%, 40.99% and 41.69% respectively compared with the traditional lead-containing protective material. Rare earth elements can greatly reduce the thickness and weight of the protective material so that they can be used as an alternative material for lead.

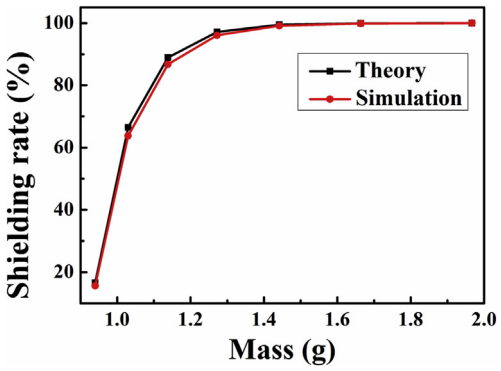

Fig. 8. Calculation and simulation curves of shielding rate change with the increasing mass.

Declaration of competing interest

There is no financial or personal interest in the subject matter or materials discussed in the manuscript.

Acknowledgements

The authors gratefully acknowledge the supports from Natural Science Foundation of China (Grant No. 51573007).

Appendix A. Supplementary data

Supplementary data to this article can be found online at https://doi.org/10.1016/j.net.2019.12.028.

References

[1] S. Nambiar, J.T.W. Yeow, Polymer-composite materials for radiation protection, ACS Appl. Mater. Interfaces 4 (11) (2012) 5717–5726.
[2] M. Hernández-Rivera, I. Kumar, S.Y. Cho, B.Y. Cheong, M.X. Pulikkathara, S.E. Moghaddam, K.H. Whitmire, L.J. Wilson, High-performance hybrid bismuth–carbon nanotube based contrast agent for X-ray CT imaging, ACS Appl. Mater. Interfaces 9 (7) (2017) 5709–5716.
[3] Y. Morishima, K. Chida, Y. Katahira, The effectiveness of additional lead-shielding drape and low pulse rate fluoroscopy in protecting staff from scatter radiation during cardiac resynchronization therapy (CRT), Jpn. J. Radiol. 37 (1) (2019) 95–101.
[4] U. Lange, A. Kluge, J. Teichmann, H. Stracke, W.S. Rau, K.L. Schmidt, Bone density measurement by dual photon absorptiometry (DPX) and single energy-quantitative computed tomography (SEQCT) in ankylosing spondylitis (AS), Aktuelle Rheumatol. 26 (1) (2001) 1–6.
[5] L.-J. Xie, J.-F. Li, F.-W. Zeng, H. Jiang, M.-H. Cheng, Y. Chen, Is bone mineral density measurement using dual-energy X-ray absorptiometry affected by gamma rays? J. Clin. Densitom. 16 (3) (2013) 275–278.
[6] N.Z.N. Azman, S.A. Siddiqui, R. Hart, I.M. Low, Microstructural design of lead oxide-epoxy composites for radiation shielding purposes, J. Appl. Polym. Sci. 128 (5) (2013) 3213–3219.
[7] S.H. Hosseini, S.N. Ezzati, M. Askari, Synthesis, characterization and X-ray shielding properties of polypyrrole/lead nanocomposites, Polym. Adv. Technol. 26 (6) (2015) 561–568.
[8] Y. Wu, Q.-P. Zhang, D. Zhou, L.-P. Liu, Y.-C. Xu, D.-G. Xu, Y.-L. Zhou, One-dimensional lead borate nanowhiskers for the joint shielding of neutron and gamma radiation: controlled synthesis, microstructure, and performance evaluation, CrystEngComm 19 (48) (2017) 7260–7269.
[9] E. Sakar, M. Buyukyildlz, B. Alim, B.C. Sakar, M. Kurudirek, Leaded brass alloys for gamma-ray shielding applications, Radiat. Phys. Chem. 159 (2019) 64–69.
[10] L. Liu, L. He, C. Yang, W. Zhang, R.G. Jin, L.Q. Zhang, In situ reaction and radiation protection properties of Gd(AA)(3)/NR composites, Macromol. Rapid Commun. 25 (12) (2004) 1197–1202.
[11] R. Sykora, V. Babayan, M. Usakova, J. Kruzelak, I. Hudec, Rubber composite materials with the effects of electromagnetic shielding, Polym. Compos. 37 (10) (2016) 2933–2939.
[12] S. Jayakumar, T. Saravanan, J. Philip, Preparation, characterization and X-ray attenuation property of Gd2O3-based nanocomposites, Appl. Nanosci. 7 (8) (2017) 919–931.
[13] S. Nambiar, E.K. Osei, J.T.W. Yeow, Polymer nanocomposite-based shielding against diagnostic X-rays, J. Appl. Polym. Sci. 127 (6) (2013) 4939–4946.
[14] P.F. Lou, X.B. Teng, Q.X. Jia, Y.Q. Wang, L.Q. Zhang, Preparation and structure of rare earth/thermoplastic polyurethane fiber for X-ray shielding, J. Appl. Polym. Sci. 136 (17) (2019).
[15] J. Kim, D. Seo, B.C. Lee, Y.S. Seo, W.H. Miller, Nano-W dispersed gamma radiation shielding materials, Adv. Eng. Mater. 16 (9) (2014) 1083–1089.
[16] S.-C. Kim, K.-R. Dong, W.-K. Chung, Performance evaluation of a medical radiation shielding sheet with barium as an environment-friendly material, J. Korean Phys. Soc. 60 (1) (2012) 165–170.
[17] H.M. Soylu, F.Y. Lambrecht, O.A. Ersoz, Gamma radiation shielding efficiency of a new lead-free composite material, J. Radioanal. Nucl. Chem. 305 (2) (2015) 529–534.
[18] H. Chai, X.B. Tang, M.X. Ni, F.D. Chen, Y. Zhang, D. Chen, Y.L. Qiu, Preparation and properties of novel, flexible, lead-free X-ray-shielding materials containing tungsten and bismuth(III) oxide, J. Appl. Polym. Sci. 133 (10) (2016).
[19] M.R. Ambika, N. Nagaiah, S.K. Suman, Role of bismuth oxide as a reinforcer on gamma shielding ability of unsaturated polyester based polymer composites, J. Appl. Polym. Sci. 134 (13) (2017).
[20] J.P. McCaffrey, E. Mainegra-Hing, H. Shen, Optimizing non-Pb radiation shielding materials using bilayers, Med. Phys. 36 (12) (2009) 5586–5594.
[21] P. Saini, V. Choudhary, Conducting polymer coated textile based multilayered shields for suppression of microwave radiations in 8.2-12.4 GHz range, J. Appl. Polym. Sci. 129 (5) (2013) 2832–2839.
[22] Y. Kim, S. Park, Y. Seo, Enhanced X-ray shielding ability of polymer–nonleaded metal composites by multilayer structuring, Ind. Eng. Chem. Res. 54 (22) (2015) 5968–5973.
[23] N. Afsarimanesh, S.C. Mukhopadhyay, M. Kruger, Sensing technologies for monitoring of bone-health: a review, Sens. Actuators A Phys. 274 (2018) 165–178.
[24] A. Milinarsky, S. Fischer, V. Giadrosich, D. Casanova, Bone mineral density by single photon X-ray absorptiometry in Chilean children and adolescents, J. Rheumatol. 25 (10) (1998) 2003–2008.
[25] O. Agar, M.I. Sayyed, F. Akman, H.O. Tekin, M.R. Kaçal, An extensive investigation on gamma ray shielding features of Pd/Ag-based alloys, Nucl. Eng. Technol. 51 (3) (2019) 853–859.
[26] D.K. Gaikwad, M.I. Sayyed, S.N. Botewad, S.S. Obaid, Z.Y. Khattari, U.P. Gawai, F. Afaneh, M.D. Shirshat, P.P. Pawar, Physical, structural, optical investigation and shielding features of tungsten bismuth tellurite based glasses, J. Non-Cryst. Solids 503–504 (2019) 158–168.
[27] M.I. Sayyed, H.O. Tekin, O. Kılıcoglu, O. Agar, M.H.M. Zaid, Shielding features of concrete types containing sepiolite mineral: comprehensive study on experimental, XCOM and MCNPX results, Results in Physics 11 (2018) 40–45.
[28] S.F. Olukotun, S.T. Gbenu, F.I. Ibitoye, O.F. Oladejo, H.O. Shittu, M.K. Fasasi, F.A. Balogun, Investigation of gamma radiation shielding capability of two clay materials, Nucl. Eng. Technol. 50 (6) (2018) 957–962.
[29] M.R. Kaçal, F. Akman, M.I. Sayyed, F. Akman, Evaluation of gamma-ray and neutron attenuation properties of some polymers, Nucl. Eng. Technol. 51 (3) (2019) 818–824.